



Published in final edited form as:

Science. 2009 February 6; 323(5915): 802–806. doi:10.1126/science.1165527.

Axon Regeneration Requires A Conserved MAP Kinase Pathway

Marc Hammarlund^{1,2,3,*}, Paola Nix^{1,*}, Linda Hauth¹, Erik M. Jorgensen^{1,2}, and Michael Bastiani¹

¹Department of Biology, University of Utah 257 South 1400 East, Salt Lake City, Utah 84112-0840, USA.

²Howard Hughes Medical Institute, University of Utah 257 South 1400 East, Salt Lake City, Utah 84112-0840, USA.

Abstract

Regeneration of injured neurons can restore function, but most neurons regenerate poorly or not at all. The failure to regenerate in some cases is due to a lack of activation of cell-intrinsic regeneration pathways. Thus, these pathways might be targeted for the development of therapies that can restore neuron function after injury or disease. Here, we show that the DLK-1 MAP kinase pathway is essential for regeneration in *C. elegans* motor neurons. Loss of this pathway eliminates regeneration, while activating it improves regeneration. Further, these proteins also regulate the later step of growth cone migration. We conclude that after axon injury, activation of this MAP kinase cascade is required to switch the mature neuron from an aplastic state to a state capable of growth.

Keywords

regeneration; *C. elegans*; MAP kinase; DLK-1; p38

Severed neurons can regenerate. After axons are cut, neurons can extend a new growth cone from the axon stump and attempt to regrow a normal process. Most invertebrate neurons can regenerate, as can neurons in the mammalian peripheral nervous system. By contrast, neurons in the mammalian central nervous system have limited regenerative capability (1). Regeneration is thought to be initiated by signals arising from the injury, including calcium spikes and the retrograde transport and nuclear import of regeneration factors (2). These mechanisms lead to increased cAMP levels, local and somatic protein synthesis, and changes in gene transcription, that in turn promote remodeling of the cytoskeleton and plasma membrane at the site of injury. The ability of specific neurons to regenerate is determined in part by the balance between pro-regeneration signals and cellular pathways that inhibit regeneration. For example, regeneration in the mammalian CNS is inhibited by extrinsic signals from myelin and chondroitin sulfate proteoglycans (CSPGs); these signals activate pathways in the damaged neuron that prevent regrowth (3). But CNS regeneration can be achieved even in the presence of inhibitory signals. A conditioning lesion to a peripheral process results in increased regeneration of the CNS branch of dorsal root ganglion neurons, presumably by triggering injury signals that result in an overall increase in regenerative potential (4). Thus,

Correspondence should be directed to bastiani@bioscience.utah.edu.

³Current address: Department of Genetics and Program in Cellular Neuroscience, Neurodegeneration and Repair, Yale University School of Medicine, 295 Congress Ave., New Haven, Connecticut 06510.

*These authors contributed equally to this work

Abbreviations: CNS, CSPG, GABA, MAPKKK, MAPKK, MAPK, HS, OE

intrinsic regeneration signals can influence regenerative success, and these signaling processes represent potential targets for therapies to enhance regeneration.

We identified the MAP kinase kinase kinase (MAPKKK) *dlk-1* as essential for regeneration in the course of a large screen for genes required for axon regeneration. The screen was conducted in a β -spectrin mutant background (5). Neurons in β -spectrin mutants break due to mechanical strain induced by locomotion. The GABA motor neurons respond to breaks by regenerating toward their targets in the dorsal cord (6). Axon guidance during regeneration is imperfect, resulting in axons in mature animals with branching and other abnormalities (Fig. 1). We found that RNA interference of *dlk-1* eliminates regeneration. Neither *unc-70* (6) nor *dlk-1* (7) are essential for axon outgrowth during development of the GABA neurons (Fig. 1; Sup. Methods). The *unc-70 dlk-1* synthetic phenotype for axon morphology suggests that *dlk-1* may function specifically in regeneration.

To demonstrate that *dlk-1* functions in regeneration independently of *unc-70*, we used laser axotomy to trigger regeneration. The GABA motor neurons can regenerate after laser axotomy (8). We used a pulsed 440 nm laser to cut axons (9). In L4-stage wild-type animals, 70% of severed axons initiated growth cones within 24 hours after axotomy (Fig. 2, Sup. Table 1). But when axons were cut in L4-stage *dlk-1(ju476)* null mutants, growth cones were never observed. These severed neurons appeared healthy after surgery: both the stump of the remaining axon and its cell body showed no decrease in GFP expression or other signs of injury. Nevertheless, these neurons failed to regenerate. To test whether regeneration was merely delayed, we monitored some severed axons for 5 days: regeneration still was not observed. Thus, *dlk-1* is essential for axon regeneration after spontaneous breaks and after laser surgery, but is dispensable for axon outgrowth during development.

Mosaic experiments demonstrate that the DLK-1 protein acts in the damaged cell rather than in the surrounding tissue. To determine whether DLK-1 acts cell-autonomously to promote regeneration, we expressed DLK-1 under the GABA-specific promoter *Punc-47* in the *dlk-1* null background. Neurons were severed by laser surgery and regeneration assayed after 18–24 hours. We found that expressing DLK-1 in the GABA neurons restored regeneration to *dlk-1* null mutants (Fig. 2C). Further, mutations that affect DLK-1 levels also affect regeneration (Fig. 2D). In *C. elegans*, DLK-1 levels are negatively regulated by RPM-1 (7). Over expression of RPM-1 reduced regeneration after surgery to levels similar to *dlk-1* loss-of-function mutants. Conversely, initiation of regeneration was enhanced in *rpm-1* mutant animals. Initiation of regeneration was also enhanced in animals lacking FSN-1, an F-box protein that functions with RPM-1 to promote DLK-1 degradation (10). However, loss of GLO-1/Rab or GLO-4/Rab GEF, which mediate ubiquitin-independent functions of RPM-1 (10), did not have strong effects on regeneration. These results confirm that changes in DLK-1 protein abundance can determine regenerative ability.

Although regeneration is age-dependent, *dlk-1* is required at all stages and over expression of DLK-1 can rescue some age dependent decline (Fig 2E). We analyzed regeneration at various developmental stages. We found that regeneration declines significantly with age, and only a few axons in old adults regenerated (9). Despite these differences, *dlk-1* is required for all regeneration, even in very young animals. Because growth cones in the young animals had not yet reached their targets, the dependence on *dlk-1* is not correlated with target contact or synaptogenesis. Further, *dlk-1* is required for regeneration of both presynaptic and postsynaptic processes (Sup. Methods).

To mediate regeneration, DLK-1 is required at the time of injury (Fig. 2F). We expressed the DLK-1 protein at different times using the heat shock promoter *Phsp-16.2*. DLK-1 expression at the time of injury was sufficient for regeneration. Applying heat shock hours before or hours

after surgery resulted in less regeneration, and when heat shock was applied either 11 hours before or 48 hours after surgery, little or no regeneration was observed. This effect was independent of age, because surgery in L2-stage larvae failed to elicit regeneration when heat shock was applied 48 hours later. Thus, DLK-1 must function within a short temporal window near the time of surgery to mediate regeneration, rather than establishing a permissive state for regeneration during development. These data suggest that DLK-1 signaling must coincide with other pro-regeneration signals, such as calpain activation (11) or cAMP elevation (12–14), for regeneration to occur.

DLK-1 is required for growth cone formation rather than the earlier step of filopodial extension. We used time-lapse microscopy to monitor morphological changes in axons after surgery. We found that in wild-type animals, newly-severed axons repeatedly extend short, transient filopodia from the axon stump (Fig. 3, Sup. Movie 1). The first filopodium appears with an average delay of more than three hours. In animals that successfully initiate regeneration a single filopodium eventually persists and is transformed into a growth cone. Growth cone formation in wild-type animals occurs with an average delay of 7 hours after surgery. In *dlk-1* mutants, transient filopodia appear at approximately the same time and the same rate as in the wild type. However, growth cones were never observed in these mutants. These data demonstrate that DLK-1 is required to transform exploratory filopodia into growth cones.

Increased expression of DLK-1 in wild-type animals accelerates the formation of growth cones and improves migration success. We over expressed DLK-1 in GABA neurons and found that time of growth cone initiation by axon stumps was advanced relative to the wild type (Fig. 3, Sup. Movie 3). Also, more axons initiated growth cones (Fig. 4). In addition to these effects on growth cone initiation, DLK-1 over expression improved growth cone performance. In wild-type animals, regenerating growth cones often have a branched, dystrophic morphology. Dystrophic growth cones migrate poorly, and most never reach the dorsal nerve cord in 24 hours (Fig. 3). These dystrophic growth cones resemble dystrophic growth cones observed in failed regeneration in the mammalian CNS (15). By contrast, regenerating growth cones in neurons that over express DLK-1 have a compact shape, similar to growth cones observed during initial axon development (16). These compact growth cones were much more likely to reach the dorsal nerve cord. Growth cone migration during regeneration in *C. elegans* shares some genetic requirements with developmental axon guidance, including components of the netrin and slit signaling pathways (17) and the ephrin pathway (9). It is possible that DLK-1 over expression improves regeneration by affecting the response of the growth cone to such signals. Thus, DLK-1 acts at two steps of regeneration: it is required for growth cone formation, and it also controls growth cone morphology and behavior.

DLK-1 functions in a MAP kinase signaling cascade that also includes the MAP kinase kinase (MAPKK) MKK-4, and the p38 MAP kinase (MAPK) PMK-3 (7). We tested whether this entire MAP kinase signaling module functions in regeneration by examining null mutants in *mkk-4* and *pmk-3*. Like *dlk-1*, neither of these mutants has appreciable defects in axon outgrowth during development. But after axotomy, both mutant strains fail to initiate regeneration (Fig. 4A). These data suggest that MKK-4 and PMK-3 are the downstream targets of DLK-1 for regeneration. Inhibition of p38 also reduces regeneration of cultured vertebrate neurons (18), suggesting that the function of p38 MAP kinases in regeneration is conserved. Do other MAP kinase cascades also contribute to regeneration? We tested a sampling of *C. elegans* MAP kinase components and found that mutations in these genes did not eliminate regeneration (Fig. 4B). Initiation of regeneration was not affected by loss of the MAPKKK *nsy-1* or its target MAPKK *sek-1*. Loss of the MAPKK *jkk-1* also did not affect regeneration. By contrast, loss of the MAPKKK *mlk-1* reduced initiation of regeneration (although some regeneration still occurred), as did loss of its downstream target *mek-1*. MLK-1 and MEK-1 are thought to activate a second *C. elegans* p38 MAP kinase, PMK-1 (19), suggesting that

multiple p38 family members contribute to regeneration. (Since null mutations in *pmk-1* are lethal, we were unable to test its function directly.) Loss of the MAPK *jnk-1* increased initiation of regeneration. Thus, while the DLK-1/MKK-4/PMK-3 MAP kinase cascade is required to initiate regeneration, other MAP kinase pathways also regulate this process. Consistent with these data, mutations in *mkk-4* or *pmk-3* did not eliminate the stimulation of regeneration by DLK-1 over expression, suggesting that crosstalk between MAP kinase modules may contribute to regeneration (Fig. 4C). However, the modest phenotype of other MAP kinase mutants, and the inability of DLK-1 over expression to bypass the requirement for *mkk-4* and *pmk-3*, suggest that the DLK-1/MKK-4/PMK-3 module is the major MAP kinase pathway for axon regeneration.

What stimulates DLK-1 function when an axon breaks? In the simplest model, the axon break interrupts trafficking of DLK-1. Local DLK-1 accumulation in the injured neuron then leads to homodimerization and activation, followed by activation of the downstream targets MKK-4 and PMK-3 (Fig. 4D). Alternatively, specific regulatory mechanisms activate DLK-1 after injury, such as scaffolding proteins like Jip1 (20), phosphatases such as PP1, PP2a, and calcineurin (21), or regulators of the proteasome (22). The strict requirement for the DLK-1 pathway in regeneration suggests that mature neurons have intrinsic barriers to growth that are not present during development. Once axons have reached their target and begun synaptogenesis, termination of growth signals by mechanisms like RPM-1 may down regulate growth to allow synapse maturation and to stabilize neuronal architecture. Indeed, mutations in RPM-1 or its homologs cause overgrowth of axons in worms (23), aberrant sprouting in *Drosophila* (24), and aberrant growth cone initiation on axon shafts in mouse (25). We found that *dlk-1* is required for regeneration even in neurons that are actively growing at the time of injury. Further, over expressing DLK-1 partially prevented the loss of regeneration in old animals (Fig. 2E). Thus, barriers to growth are quickly erected in axons, and post-injury signaling via DLK-1, MKK-4, and PMK-3 is required to drive the neuron back to its prelapsarian, embryonic state.

How does the MAP kinase PMK-3 stimulate regeneration? The DLK-1 pathway is first required for growth cone formation about 7 hours after a break occurs—a process likely to be mediated by the polymerization of microtubules. Activated p38 MAP kinase regulates microtubule dynamics (25), and microtubule remodeling is required for growth cone initiation during regeneration (26). Further, defects in microtubule dynamics contribute to the axon outgrowth phenotype of *Phr1* mutant mice (25). Activated p38 may also control other targets that facilitate axon regeneration. p38 regulates local protein synthesis (27), which is required for regeneration (18). p38 is also likely to have functions in the nucleus, since it contributes to injury-induced changes in gene transcription (28). Activated p38 may reach the nucleus by retrograde transport: retrograde transport in general is critical for regeneration (29) and transport of activated MAP kinases from axons to the cell body following axotomy has been observed in *Aplysia* sensory neurons (30) and in rodent sciatic nerves (31,32). Thus, regeneration may require activated PMK-3/p38 at the site of the break to regulate microtubule stability and protein expression, and also require PMK-3 to traffic to the nucleus to regulate gene transcription (Fig. 4D). The DLK-1 signaling pathway thus provides a critical link between axon injury and the process of regeneration.

Methods

Strains

Animals were maintained on NG agar plates with *E. coli* HB101 as a food source according to standard methods. See Sup. Table 1 for all strains and complete genotypes. The wild type was EG1285 *oxIs12*.

RNAi

RNAi was performed by feeding as described (1). Bleached embryos from MJB1046 *basIs1; oxIs268, unc-70(s1502); eri-1(mg366); lin-15(n765)* gravid hermaphrodites were placed on *dlk-1* RNAi bacteria. Plates were incubated at 15°C for 12–13 days. A minimum of 10 F1 L4 animals were scored by counting all GABA commissures contacting the dorsal cord. Because commissures are sometimes obscured by other processes, this method slightly underestimates the actual number. For example we typically scored 16 commissures in wild-type animals, compared to the actual number of 19.

Axotomy

L4-stage hermaphrodites were mounted in 10 mM muscimol in M9 on an agarose pad under a coverslip. GFP expressing DD and VD motor neurons were imaged with a Microradiance 2000 confocal microscope using a Nikon 60X, 1.4 NA lens. Selected commissural axons were cut using a 440 nm MicroPoint Laser System from Photonic Instruments. After surgery, animals were recovered to an agar plate, and remounted for confocal imaging approximately 18–24 hours post-surgery. The imaged commissures were classified according to the following criteria: 1) regeneration (number of commissures with well-defined growth cones present on the proximal fragment and/or a net growth of 5 μ m or more, 2) sprouting (number of commissures with small branches present on the proximal fragment), and 3) no regeneration (no change to proximal fragment after 18–24 hours). A minimum of 20 individuals (with 1–3 axotomized commissures each) were observed for most experiments.

In cases where the genetic background resulted in improved regeneration the data are likely to be an underestimate of successful regeneration. To ensure that only axons which had been completely severed were analyzed, we eliminated experiments that did not include a growth cone and/or a recognizable distal fragment after 18–24 hours. This approach underestimates successful regeneration because any experiment in which the regenerated axon obscured the distal stump would appear as an uncut commissure and would be eliminated. 95% confidence intervals were calculated by the modified Wald method, and two-tailed P values were calculated using Fisher's exact test (<http://www.graphpad.com/quickcalcs/>).

Molecular Biology

Molecular biology was done using standard techniques. PCR was done with Phusion DNA Polymerase (Finnzymes). Templates were either genomic DNA from mixed-stage N2 or first strand cDNA obtained by dT-primed reverse transcription of poly-A selected RNA from mixed-stage N2. Plasmids were assembled using multisite Gateway recombination (Invitrogen).

pPN12 (Punc-47:dlk-1 minigene)—A 5' fragment (exon 1 and 2) was amplified from genomic DNA and a 3' fragment (exons 3–11) from cDNA. The two fragments were ligated and a full-length product for generating a Gateway entry clone was obtained by amplifying with the following primers:

PN18 ggggacaagtttgtaaaaaagcaggctggacatctaccacaatggaacc

PN19 ggggaccactttgtacaagaagctgggtgaattcggactgctccggcatcg.

The final construct was obtained in a multisite Gateway reaction using the following constructs: pMH522 (*Punc-47* [4-1]), pPN11 (*dlk-1* minigene [1-2]), pMH473 (*unc-54* terminator [2-3]), and pDEST [4-3].

pPN14 (Punc-47:dlk-1 cDNA-GFP)—The genomic portion of pPN11 was replaced with a BstEII-SalI digested cDNA fragment (PN16 acatctaccacaatgtaacc, PN31 cggagcttctctgcatg). The final construct was obtained in a multisite Gateway reaction using the following constructs: pMH522 (*Punc-47* [4-1]), pPN13 (*dlk-1* cDNA [1-2]), pGH50 (GFP:*unc-54* terminator [2-3]), and pDEST [4-3].

pMH524 (Phsp-16.2:dlk-1 cDNA-mCherry)—The final construct was obtained in a multisite Gateway reaction using the following constructs: pMH520 (*Phsp-16.2* [4-1]), pPN13 (*dlk-1* cDNA [1-2]), pGH38 (mCherry:*unc-54* terminator [2-3]), and pCFJ150 MosSci [4-3].

Transgenics

Transgenic animals were obtained as described (2). MJB1011 was constructed by injecting EG4529 *oxIs268* with pPN12 DNA at 30ng/μl along with *Pmyo-2::mCherry* at 2ng/μl as a co-injection marker. MJB1032 was constructed by injecting N2 with pPN14 DNA at 30ng/μl along with *Punc-47::mCherry* at 20ng/μl. EG5203 was constructed by injecting MJB1014 *dlk-1(ju476)*; *oxIs12* with *Phsp-16-2::DLK-1-mCherry* at 5 ng/μl together with *Pmyo-2::GFP* at 2 ng/μl as an injection marker and 1 kb ladder at 50 ng/μl as carrier. Stable transgenic lines were recovered based on GFP in pharynx muscles and subjected to heat shock. Two out of three lines tested showed weak mCherry in the intestine 24 hours after heat shock, suggesting that heat shock resulted in appreciable expression of the DLK-1-mCherry fusion protein. One of these lines was used for further experiments.

Neuron Polarity

The L4-stage GABA motor neurons are of two types, DD and VD, with similar morphologies but opposite polarities (3). Axotomy at the midline therefore severs the presynaptic region of the DD neurons and the postsynaptic region of the VD neurons. We typically cut VD11, VD10, and DD5. In some genetic backgrounds or developmental stages nearly all neurons regenerated; in others, such as *dlk-1* mutants, none did. Thus, as previously reported, regeneration was similar in DD and VD neurons (4), and *dlk-1* is required in both neuron types. As an additional control we cut L1 stage identified DD axons, before VDs grew out, and compared their regeneration to identified VD axons cut during late L1. We observed no significant difference in DD regeneration compared to VD regeneration (Fig. 2E).

Development

To address a potential function for *dlk-1* in development of the DD neurons, we imaged them in L1-stage animals, before they were masked by the VD neurons. We scored 100 L1 animals and found no difference from wild type in number of commissures, branching, pathfinding errors, or other defects. We did observe a slight increase in gaps between dendrites along the dorsal cord. Although the number of gaps in the dorsal cord was not significantly different ($P = 0.1757$), there was a significant difference in average gap length, 2.3 μm (range from 1–7 μm) in the wild type and 4.4 μm (range 1–10 μm) in *dlk-1* ($P < 0.0001$).

Heat Shock

Mixed-stage animals were heat shocked at 33°C for 1 hour on a sealed worm plate in a recirculating water bath. L4-stage animals containing the *Phsp-16-2::DLK-1-mCherry* array were selected based on pharynx GFP.

Filopodia

Confocal images collected at 5-minute intervals were analyzed for the appearance of filopodia (small, transient extensions from the axon tip or shaft). Since some filopodia appear in only one frame, there are probably some even faster events that are too rapid to be captured by this

imaging protocol. Thus, our data likely underestimate the true number of transient events. 11 axons in 8 animals were analyzed for wild type and 9 axons in 5 animals for *dllk-1(ju476)*. For wild-type axons, analysis was terminated at the appearance of the filopodium that eventually stabilized into a growth cone. The average time to this event was 460 minutes.

Since *dllk-1* mutants never initiate growth cones, they continue to generate filopodia throughout the analysis, long after the average time to initiate a growth cone in wild type. Because these late events have no equivalent in wild-type animals, they were eliminated from the comparison in Figure 3G. Only events in both genotypes occurring before 460 minutes were considered. Figure 3H shows the average time and the standard error for the first event. Figure 3I shows the average rate. For this analysis, the number of filopodia observed in each axon was divided by the time of observation for that axon. Analysis was truncated at growth cone initiation or 460 minutes, whichever came first.

Time-lapse Microscopy

Methods are similar to those described (5) with the following changes. L4 worms were anesthetized with 1 μ l of 10 mM muscimol (Sigma M1523) in M9 and mounted on 5–10% agarose pads. Agarose included 0.002% 1-phenoxy-2-propanol (Janssen Chimica). Worms were cover slipped and the slide sealed in Vaseline to prevent evaporation. Axotomy was performed as described above, and time lapse images were collected (Lasersharp 2000) every 5 min. over a Z range of 10–15 μ m at 0.1 μ m/pixel resolution. Maximum projections of each time point were exported to ImageJ for analysis.

Supplementary Material

Refer to Web version on PubMed Central for supplementary material.

References

1. Case LC, Tessier-Lavigne M. *Curr Biol* 2005;15:R749. [PubMed: 16169471]
2. Rossi F, Gianola S, Corvetto L. *Prog Neurobiol* 2007;81:1. [PubMed: 17234322]
3. Liu BP, Cafferty WB, Budel SO, Strittmatter SM. *Philos Trans R Soc Lond B Biol Sci* 2006;361:1593. [PubMed: 16939977]
4. Neumann S, Woolf CJ. *Neuron* 1999;23:83. [PubMed: 10402195]
5. Hammarlund M, Davis WS, Jorgensen EM. *J Cell Biol* 2000;149:931. [PubMed: 10811832]
6. Hammarlund M, Jorgensen EM, Bastiani MJ. *J Cell Biol* 2007;176:269. [PubMed: 17261846]
7. Nakata K, et al. *Cell* 2005;120:407. [PubMed: 15707898]
8. Yanik MF, et al. *Nature* 2004;432:822. [PubMed: 15602545]
9. Wu Z, et al. *Proc Natl Acad Sci USA*. 2007
10. Grill B, et al. *Neuron* 2007;55:587. [PubMed: 17698012]
11. Gitler D, Spira ME. *J Neurobiol* 2002;52:267. [PubMed: 12210094]
12. Chierzi S, Ratto GM, Verma P, Fawcett JW. *Eur J Neurosci* 2005;21:2051. [PubMed: 15869501]
13. Neumann S, Bradke F, Tessier-Lavigne M, Basbaum AI. *Neuron* 2002;34:885. [PubMed: 12086637]
14. Qiu J, et al. *Neuron* 2002;34:895. [PubMed: 12086638]
15. Silver J, Miller JH. *Nat Rev Neurosci* 2004;5:146. [PubMed: 14735117]
16. Knobel KM, Jorgensen EM, Bastiani MJ. *Development* 1999;126:4489. [PubMed: 10498684]
17. Gabel CV, Antonie F, Chuang CF, Samuel AD, Chang C. *Development* 2008;135:1129. [PubMed: 18296652]
18. Verma P, et al. *J Neurosci* 2005;25:331. [PubMed: 15647476]
19. Ewbank JJ. *WormBook* 2006:1. [PubMed: 18050470]
20. Nihalani D, Meyer D, Pajni S, Holzman LB. *EMBO J* 2001;20:3447. [PubMed: 11432832]

21. Mata M, Merritt SE, Fan G, Yu GG, Holzman LB. *J Biol Chem* 1996;271:16888. [PubMed: 8663324]
22. Daviau A, et al. *J Biol Chem* 2006;281:31467. [PubMed: 16931512]
23. Schaefer AM, Hadwiger GD, Nonet ML. *Neuron* 2000;26:345. [PubMed: 10839354]
24. Collins CA, Wairkar YP, Johnson SL, DiAntonio A. *Neuron* 2006;51:57. [PubMed: 16815332]
25. Lewcock J, Genoud N, Lettieri K, Pfaff S. *Neuron* 2007;56:604. [PubMed: 18031680]
26. Erez H, et al. *J Cell Biol* 2007;176:497. [PubMed: 17283182]
27. Campbell DS, Holt CE. *Neuron* 2003;37:939. [PubMed: 12670423]
28. Zroui H, Le Goascogne C, Li WW, Pierre M, Courtin F. *Eur J Neurosci* 2004;20:1811. [PubMed: 15380002]
29. Hanz S, Fainzilber M. *J Neurochem* 2006;99:13. [PubMed: 16899067]
30. Sung YJ, Povelones M, Ambron RT. *J Neurobiol* 2001;47:67. [PubMed: 11257614]
31. Perlson E, et al. *Neuron* 2005;45:715. [PubMed: 15748847]
32. Reynolds AJ, Hendry IA, Bartlett SE. *Neuroscience* 2001;105:761. [PubMed: 11516839]
33. This work is dedicated to the memory of Craig H. Neilsen. We thank Chi-Bin Chen, Dave Gard, Wayne Davis, Jamie White and Kim Schuske for helpful discussions. Supported by the Craig H. Neilsen Foundation, the McKnight Endowment Fund for Neuroscience and NIH 1R21NS060275 to MB and NIH NS034307 to EMJ.

References

1. Kamath RS, et al. *Nature* 2003;421:231. [PubMed: 12529635]
2. Mello CC, Kramer JM, Stinchcomb D, Ambros V. *EMBO J* 1991;10:3959. [PubMed: 1935914]
3. White JG, Southgate E, Thomson JN, Brenner S. *Phil. Trans. Royal Soc. London* 1986;314:1.
4. Wu Z, et al. *Proc Natl Acad Sci USA*. 2007
5. Knobel KM, Jorgensen EM, Bastiani MJ. *Development* 1999;126:4489. [PubMed: 10498684]

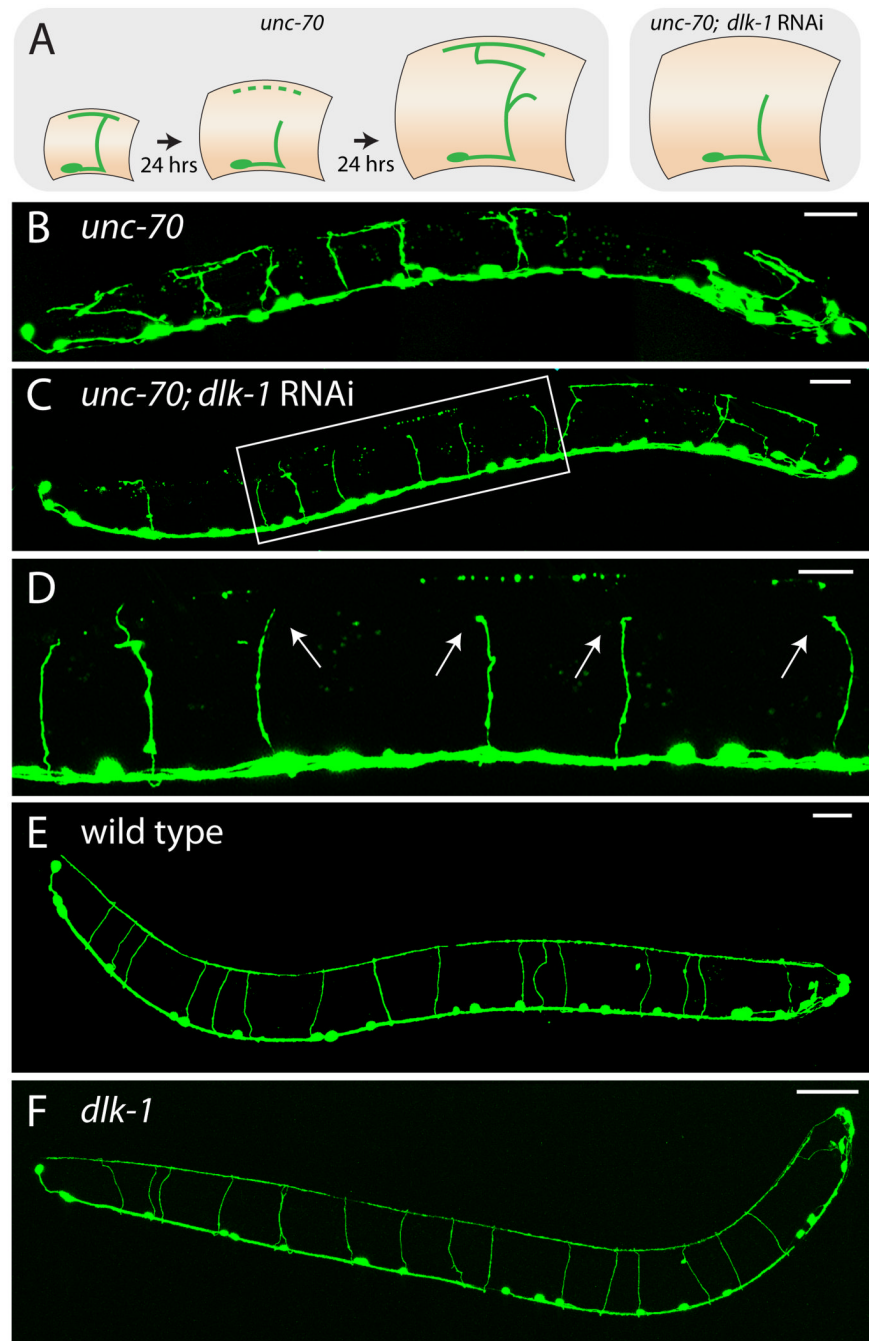


Fig. 1. *dlk-1* is required for axon regeneration in β -spectrin mutants. (A) Cartoon showing development of axon morphology in control β -spectrin mutant (left) and in β -spectrin mutant lacking hypothetical regeneration gene (right). (B and C) GABA neurons in representative L4-stage β -spectrin mutants (*unc-70*) under control conditions or after *dlk-1* RNAi. Scale bars: 20 μ m. (D) High-magnification view of boxed region in (C). Arrows indicate inert axon stumps. Scale bar: 10 μ m. (E and F) GABA neurons in representative L4-stage wild-type and *dlk-1* mutant animals. Scale bars: 20 μ m.

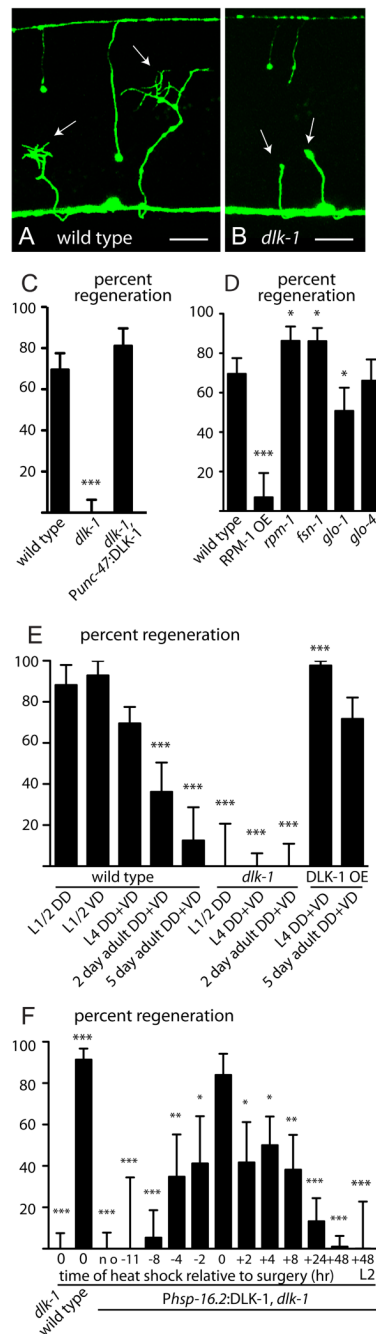


Fig. 2. *dlk-1* is required in severed axons for growth cone initiation. (A) Regenerating axons 18–20 hours after laser surgery in a wild-type animal. Both severed axons have generated a growth cone (arrows). Scale bar: 10 μ m. (B) Axons in *dlk-1* mutants fail to generate growth cones 18–24 hours after surgery. Scale bar: 10 μ m. (C) DLK-1 acts cell intrinsically to mediate regeneration. (D) RPM-1 controls DLK-1 activity in axon regeneration. (E) Regeneration requires *dlk-1* at all ages and over expression of DLK-1 rescues age-associated decline. (F) DLK-1 acts at the time of injury to mediate regeneration. Time of heat shock relative to surgery is indicated in hours. No heat shock is indicated by ‘no’. ‘L2’ indicates surgery at L2-stage.

Bars in panels C–F show percentage of axons that initiated regeneration and 95% confidence interval (CI).

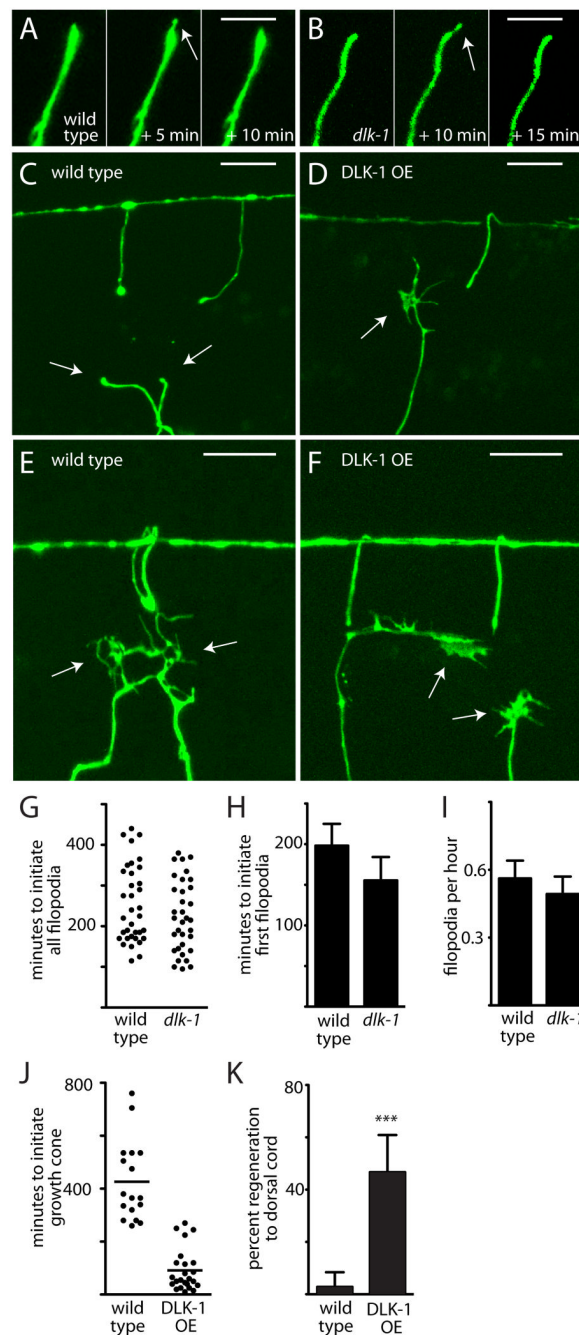


Fig. 3. *dlk-1* controls growth cone initiation and morphology during axon regeneration. **(A)** Transient filopodium in a wild-type animal. Images were taken at 165 (left), 170 (center), and 180 (right) minutes after surgery. Scale bar: 5 μ m. **(B)** Transient filopodium in a *dlk-1* mutant animal. Images were taken at 475 (left), 480 (center), and 490 (right) minutes after surgery. Scale bar: 5 μ m. **(C)** Representative axons in a wild-type animal 120 minutes after axotomy. Proximal and distal ends have retracted away from site of surgery, but proximal ends (arrows) show no evidence of regeneration. Scale bar: 10 μ m. **(D)** A representative axon in an animal over expressing DLK-1 120 minutes after axotomy. The proximal end (arrow) has already regenerated past the retracted distal end. Scale bar: 10 μ m. **(E)** Representative growth cones

in a wild-type animal. Although these axons successfully initiated regeneration, the growth cones (arrows) have a dystrophic morphology. Scale bar: 10 μm . **(F)** Representative growth cones in an animal over expressing DLK-1 under the *unc-47* promoter. These growth cones (arrows) have a compact morphology similar to growth cones observed during development. Scale bar: 10 μm . **(G)** Distribution of all times of filopodia initiation in wild type and *dlk-1*. Each dot represents a filopodium. **(H)** Time of first filopodium initiation in wild type and *dlk-1*. Bars show mean and standard error. **(I)** Rate of filopodia initiation in wild type and *dlk-1*. Bars show mean and standard error. **(J)** Time to initiate regeneration after surgery in wild type and *dlk-1* over expressing (OE) animals. Initiation is defined as the appearance of the filopodia that becomes a growth cone. Each dot represents a single axon. **(K)** Percentage of regenerating axons that reached the dorsal cord after 18–24 hours. Error bars indicate 95% CI.

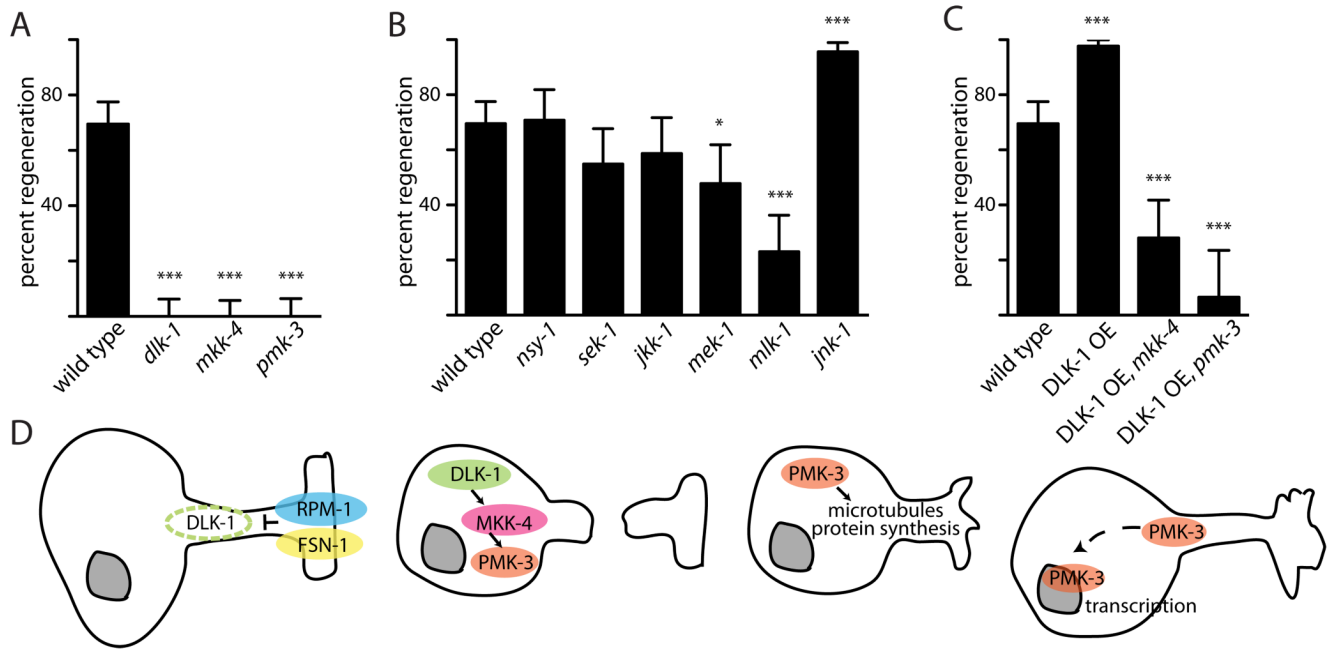


Fig. 4. MAP kinase signaling is required for axon regeneration. **(A)** Regeneration is eliminated by mutations in the DLK-1/MKK-4/PMK-3 MAP kinase module. **(B)** Other MAP kinase elements contribute to regeneration, but are not essential. **(C)** Activated DLK-1 has targets in addition to MKK-4 and PMK-3. **(D)** Model for function of MAP kinase signaling during axon regeneration.